https://doi.org/10.14669/AM/204802

MANEUVERABILITY AND MOVEMENT STABILITY OF THE BUS TRAIN BASED ON THREE "BOHDAN" BUSES

ROMAN MARCHUK[1], VOLODYMYR SAKHNO[2], IHOR MUROVANYI[3], VIKTOR POLIAKOV[4], SVITLANA SHARAI[5], NAZAR MARCHUK[6]

Abstract

The paper focuses on selected issues in modern public transport systems, which are increasingly seen as an important means of enhancing safe populations mobility, especially in urban areas suffering from growing traffic congestion. This is facilitated by the introduction of a new bus traffic system "Bus Rapid Transport" (BRT), which is the result of the bus public transport network development. The rolling stock used in the BRT system is of two types: the first one is a classic, two-link or three-link metrobus with an engine that runs on both diesel and gas fuel, as well as a hybrid electro-gas engine. These options are inherent to articulated buses, 18 and 24 meters in length. The second type is a bus train consisting of a bus and one or two trailers, or one or two buses. Therefore, the purpose of the studies is the possibility of creating a bus train based on three "Bohdan" buses. Special attention is paid to the maneuverability and movement stability, taking into account specific bus characteristics in large cities. For this purpose, the bus train consisting of three similar buses mathematical model was improved, with which the maneuverability and movement stability are determined.

1 Department of Automobiles and Automotive industry, National University of Water and Environmental Engineering, Rivne, Ukraine, e-mail: r.m.marchuk@nuwm.edu.ua, ORCID: 0000-0002-9974-8769

2 Automobiles Department, National Transport University, Kyiv, Ukraine, e-mail: sakhno@ntu.edu.ua, ORCID: 0000-0002-5144-7131

3 Faculty of Transport, Lutsk National Technical University, Lutsk, Ukraine, e-mail: igor_lntu@ukr.net, ORCID: 0000-0002-9749-980X

4 Automobiles Department, National Transport University, Kyiv, Ukraine, e-mail: poljakov_2006@ukr.net, ORCID: 0000-0001-7042-3066

5 Department of International Transportation and Customs Control, National Transport University, Kyiv, Ukraine, e-mail: svetasharai@gmail.com, ORCID: 0000-0001-6568-4990

6 Department of Automobiles and Automotive industry, National University of Water and Environmental Engineering, Rivne, Ukraine, e-mail: n.m.marchuk@nuwm.edu.ua, ORCID: 0000-0002-7439-7229

https://doi.org/10.14669/AM/204802

It was established that during the road train circular movement and the first bus steering wheels turning at the place where trailer links maximum displacement is achieved, the overall traffic lane width will be 6.7 m, which is much less than the permissible one, that is, the maneuverability of a bus train based on three "Bohdan" buses is not a limiting factor for its operation on urban routes.

Keywords: bus train; maneuverability; stability; overall traffic lane width; mathematical model

1. Introduction

Modern public transport systems are increasingly seen as an important means of safely increasing mobility, especially in urban areas suffering from growing traffic congestion. Many high-income cities have a particularly strong policy of reducing the use of private road transport through investment in public transport. Investment in safe public transport is also seen as a mechanism to promote physical activity and thus contribute to the health of the population [14].

As of early 2023, "Bus Rapid Transport" (BRT systems) have been implemented in 186 cities on six continents, comprising 5607 km of lines and serving 31.5 million passengers daily. The largest number of passengers in Latin America is 17.5 million in 62 cities [14].

The metrobus or new BRT system is a result of the development of public transport. Compared to the subway, this project has clear advantages: lower cost of network creation, lower cost of rolling stock, mobility, etc. The metrobus main advantage is its complete isolation on the road from other modes of transport.

The rolling stock used in the BRT system is of two types: the first one is a classic, two-link or three-link metrobus with an engine that runs on both diesel and gas fuel, as well as hybrid electro-gas engine. These options are inherent to articulated buses, 18 and 24 meters in length [14]. The second type is a bus train consisting of a bus and one or two trailers, or one or two buses.

Along with the undeniable advantages of three-section articulated buses, it has disadvantages – worse maneuverability compared to trailed ones. Furthermore, the efficiency of articulated buses is closely linked to passenger traffic, which can change over the course of a day. This problem can be solved by using a passenger road train with two or three buses. There is a bus train at peak hour and in the period between peaks, each bus separately (it is possible to park one bus on the designated area).

However, the use of three-link trailed road trains requires solving certain kinds of problems, in particular maneuverability, which determines the fit of such road train into the street network, as well as the movement stability.

https://doi.org/10.14669/AM/204802

The maneuverability and movement stability of road trains are determined by a combination of operational, mass-geometric and structural parameters of its modules. In general, the desired ratios of these parameters are different even for the same vehicle over a range of operating loads and speeds. As a consequence, there is the difficulty of obtaining at the early stages of road trains construction precise design parameters and quantitative indicators on the criteria of maneuverability and movement stability [14].

The modular approach to modeling presented in [12] allows for the construction of compact non-holonomic kinematic models of multi-link buses, which include an active bus and an arbitrary number of trailers connected by passive rotational joints and fixed or steered trailer wheels. In [6], the results of a comprehensive study on the stability of a linearized single-track model of a two-section articulated vehicle in a plane-parallel motion are presented. The two parts of the vehicle model are connected at the coupling point using an original hinge. The equations of motion are derived in analytical form, allowing for the study of nonlinear models (nonlinear viscoelastic characteristics of the joint). The most important parameters controlling the onset of stability disturbances are identified, as well as the role of the equivalent rotational damping coefficient and equivalent torsional stiffness characterizing the joint, in order to find criteria for its design. In [5], a unified model is proposed that includes the dynamics of the rotation of an articulated vehicle and the rotation about any axles of both the tractor vehicle (bus) and the trailer section. The model represents all possible existing configurations of buses, including articulated joints, power unit placement, and active chassis layout. For model development, three layers of the modeling process are presented step by step. The interaction of the tire with the bearing area is described by the formula, taking into account the change in vertical load. The articulated bus is represented as a system of differential equations. Model validation showed the expediency, efficiency, and convenience of the proposed approach, which can be adapted for any articulated vehicle in determining stability parameters in straight-line motion. In [20], a single-track dynamic model of an articulated bus is presented, based on the assumption that the lateral accelerations of the body front part and the turning angles of the articulated bus are small. Additionally, friction and clearances in the hinge coupling are not considered. The system is designed to accurately describe the vehicle forward and rotational motion based on differential equations of kinematic parameters representing articulated buses. Matlab-Simulink was used to solve the equations. The modeling results are functions of kinematic and dynamic parameters, allowing the trajectory and overall traffic lane width of the articulated bus to be determined. The obtained results form the basis for an accurate assessment of the dynamic model and the study of the articulated bus dynamics at a higher and more complex level. In [16], three-dimensional dynamic vehicle and trailer models have been developed, based on which train dynamic model was built. The results of the studies show that for nonlinear and linear models, the critical speeds differ little from each other. In [3], the vehicle vertical and lateral dynamics equations with 6 degrees of freedom are reduced to matrix form. The movement of such a vehicle in the vertical and lateral planes was studied. It was shown that the developed method can be applied to analyze the movement stability, in particular of passenger

https://doi.org/10.14669/AM/204802

trains. In [4], a multivariate extension of the D2-IBC (Data-Driven – Inversion-Based Control) method is considered and its application to control the road train movement stability in both straight and curved motion is discussed in detail. In [2], a simplified analysis of the vehicle combinations maneuverability and movement stability, such as a towing vehicle in combination with one or two semi-trailers or road train with a full trailer, is carried out. Vehicle combinations with trailers and semi-trailers are considered as linear dynamic systems with two degrees of freedom for each unit. The equations of motion, taking into account the influence of deceleration and acceleration, are derived, and the characteristic equation of motion at constant speed is obtained. In [17], three-dimensional linear and nonlinear dynamic models of a vehicle and trailer were built, based on which a dynamic model of a train was developed. Numerous results show that for nonlinear and linear models, the critical speeds are almost indistinguishable from each other. In [7], it is shown that heavy trucks with a large number of trailers (MTAHV) exhibit unstable modes of motion at high speeds, including folding of links, swinging the trailer and rollover, which depend on the combination of operational, mass-geometric and design parameters of the modules and their control system. The desired combinations of these parameters in terms of stability of the same vehicle in the range of operating loads and speeds are not the same. This causes difficulty in obtaining ready-made design parameters and quantitative indicators of a vehicle at the early stages of its creation according to the criteria of movement stability. In [10], the equations of a vehicle vertical and lateral dynamics were obtained and it was proven that such a method can be applied to analyze not only vehicle movement stability but also of a road trains.

Unlike articulated vehicles, the kinematic model of trailed road train is more complex [1, 11, 13]. More complex equations of trailed road train with steered trailers can be interpreted as virtual steering wheels located on the trailers, with a turning angle that is a nonlinear feedback from the output state of the configuration. The multi-chain form available for this latter system can also be restored for a general multi-link road train if additional steering inputs are replaced by feedback loops, the obtaining of which presents a new complex task. The success in solving such problems depends on how successfully the mathematical model and its essential parameters describing the behavior of the dynamic system in various modes are chosen [9, 18, 19].

The road train curvilinear movement is characterized by such parameters as speed, turning radius and steering wheels angles that do not remain constant during road train operation. Therefore, both kinematic and dynamic indicators are used to assess the vehicle maneuverability [14].

Dynamic indicators are supplied by three buses in traction mode.

The kinematics should provide:

the overall traffic lane width, equal to the difference between the external and internal overall turning radius. Given that the overall turning radius are normalized [14], R_{eo} = 12.5 m, R_{io} = 5.3 m, the overall traffic lane width, W_o = 7.2 m will also be normalized,

- ability to reverse.

https://doi.org/10.14669/AM/204802

The least studied issue to date is the possibility of reversing road trains, which was almost not considered in theory for three-link road trains. However, for a three-link road train consisting of three buses, the issue of reversing may be resolved if it is assumed that the last bus driving when reversing is the traffic parameters of the last two buses are determined by the traffic parameters of that bus. In addition, such bus train moves on separate designated lanes where reversing is almost impossible [14]. Therefore, to determine maneuverability parameters it is sufficient to have simpler kinematic models and for stability, kinematic models supplemented by forces and moments acting on individual links of the road train.

Such models are used for non-steered and steered road trains (by folding angles) are listed in the work [14]. However, for a three-link road train consisting of three buses with their own autonomous control systems, some correction of existing models is necessary (steered wheels turning of the second and third buses is performed both depending on turning angle of the first bus steered wheels and folding angles of the road train links) to determine the road train maneuverability and its ability to fit into the urban network, and sufficient conditions for movement stability. In this connection, the purpose of the work is to determine the maneuverability and movement stability indicators for a road train consisting of three buses, by carrying out typical maneuveres, ensuring that such a road train fits into the street network with movement stability.

2. Materials and Methods

In the development of a mathematical model of a road train, we use equations for both a freight and passenger road train consisting of a towing vehicle and two trailers, one of which is steered and the other is non-steered [14]. Note that the mass, moment of inertia about the vertical axis and wheelbase of all three buses are the same, i.e., $m_1 = m_2 = m_3 = m$; $I_1 = I_2 = I_3 = I$; $l_1 = l_2 = l_3 = l$. Each bus has an autonomous steering control system, with the first bus being directly controlled by the driver, and the second and third buses being controlled by their own systems, kinematically linked to the control system of the first bus and correcting of steered wheels turning angle based on folding angle Taking this into account, the equations of plane-parallel movement for the generalized coordinates – longitudinal velocity V, lateral velocity U, and angular velocity ω (yaw rate) of the road train consisting of three buses, as shown in Figure 1, were obtained by the section method and written in the form (1–13), where the following designations are used:

m_1 – mass of the first bus steering wheel module, kg;
m – mass of the first, second and third bus, kg;
V_i, U_i – longitudinal and lateral velocity of the i-th bus, m/s;
ω_i – angular velocity (yaw rate) of the i-th bus, rad/s;
θ, θ_1, θ_2 – turning angles of the first bus steering wheel module, steered wheels of second and third buses, rad;
φ_i – folding angles of the road train links, rad;

https://doi.org/10.14669/AM/204802

X_1, Y_1 – longitudinal and lateral reactions of the first bus steering wheel module, N;
XB, YB; XC, YC; XD, YD; XE, YE – longitudinal and lateral reaction at the coupling points of the road train links, N;
X_{12} – longitudinal reaction on the driving axle of the first bus, N;
X_{21}, Y_{21}; X_{22};Y_{22}; X_{31}; Y_{31}; X_{32}; Y_{32}; X_{41}; Y_{41}; X_{42}; Y_{42} – longitudinal and lateral reaction on the axles of the first, second and third buses, N.

$$-m_1(\dot{V}_1 - \omega_1 U_1) - X_1 \cos\theta_1 - Y_1 \sin\theta_1 = 0 \quad (1)$$
$$-m_1(\dot{U}_1 + \omega_1 V_1) + X_1 \sin\theta_1 - Y_1 \cos\theta_1 = 0 \quad (2)$$
$$-m(\dot{V}_2 - \omega_2 U_2) + XB - XC\cos\varphi_1 + X_{12} + YC\sin\varphi_1 = 0 \quad (3)$$
$$-m(\dot{U}_2 + \omega_2 V_2) + YB - XC\sin\varphi_1 - YC\cos\varphi_1 = 0 \quad (4)$$
$$-m(\dot{V}_3 - \omega_3 U_3) + XC + XD\cos\varphi_2 - X_{21}cos\theta_1 - X_{22}cos\varphi_2 + Y_{21}sin\theta_1 + YD\sin\varphi_3 = 0 \quad (5)$$
$$-m(\dot{U}_3 + \omega_3 V_3) + YC - YD\sin\varphi_2 + Y_{21}sin\theta_1 + Y_{22}sin\varphi_2 + X_{21}cos\theta_1 - YD\cos\varphi_3 = 0 \quad (6)$$
$$-m(\dot{V}_4 - \omega_4 U_4) + XE - X_{31}cos\theta_2 - X_{32}cos\varphi_4 + Y_{31}sin\theta_2 = 0 \quad (7)$$
$$-m(\dot{U}_4 + \omega_4 V_4) + YE + Y_{31}cos\theta_2 + Y_{32}sin\varphi_4 + X_{31}sin\theta_2 = 0 \quad (8)$$

After determining the longitudinal and lateral forces on the axles of the road train links, the longitudinal, lateral and angular velocities of the links, the system of equations was written in the form and the following designations are additional used in equations (9–13) and Figure 1:

$\beta = \varphi_1 + \varphi_2$; $\beta_1 = \varphi_1 + \varphi_3 + \varphi_4$; $\beta_2 = \varphi_3 + \varphi_4$; $\beta_3 = \varphi_1 + \varphi_3$; $\dot{\gamma} = \omega - \dot{\varphi}_1$; $\ddot{\gamma} = \dot{\omega} - \ddot{\varphi}_1$;
$\dot{\gamma}_1 = \omega - \dot{\varphi}_1 - \dot{\varphi}_2$; $\ddot{\gamma}_1 = \dot{\omega} - \ddot{\varphi}_1 - \ddot{\varphi}_2$; $\dot{\beta}_1 = \dot{\varphi}_1 + \dot{\varphi}_3 + \dot{\varphi}_4$; $\ddot{\beta}_1 = \ddot{\varphi}_1 + \ddot{\varphi}_3 + \ddot{\varphi}_4$;
I – the bus central moment of inertia relative to the vertical axis, kgm2;
ϑ_i – course angles of the road train links, rad;
$M_{ki} = f(\varphi_{ki}, \dot{\varphi}_{ki})$ – turning resistance moments of metrobus links, Nm;
a – distance from the front axle to the bus centre of mass, m;
b –distance from the rear axle to the bus centre of mass, m;
c – distance from the bus centre of mass to the coupling point with the first trailer, m;
d – distance from the coupling point with the previous link to the front axle of the bus, m;
l – wheel base, m.

$$3m(\dot{v} - u\omega) + 2c\omega^2 m - m(d+l)[\ddot{\gamma}sin\varphi_1 + \dot{\gamma}^2 cos\varphi_1] - md[\ddot{\gamma}sin\beta - \dot{\gamma}_1^2 cos\beta] + m(d + l)[\ddot{\gamma}_1 sin\beta_3 + \dot{\gamma}_1^2 cos\beta_3] - md\left[(\dot{\omega} - \ddot{\beta}_1)sin\beta_1 + (\omega - \dot{\beta}_1)^2 cos\beta_1\right] = -(X_1 cos\theta_0 - Y_1 sin\theta_0) + X_{12} - X_{31}\,cos(\theta_1 + \beta) + Y_{31}sin(\theta_1 + \beta) + X_{32} + X_{41}\,cos(\theta_2 + \beta_1) + Y_{41}sin(\theta_2 + \beta_1) + X_{42} \quad (9)$$

$$3m(\dot{u} - v\omega) - 2c\omega^2 m - m(d+l)[\ddot{\gamma}cos\varphi_1 + \dot{\gamma}^2 sin\varphi_1] - md[\ddot{\gamma}cos\beta - \dot{\gamma}_1^2 sin\beta] - m(d + l)[\ddot{\gamma}_1 cos\beta_3 + \dot{\gamma}_1^2 sin\beta_3] - md\left[(\dot{\omega} - \ddot{\beta}_1)cos\beta_1 + (\omega - \dot{\beta}_1)^2 sin\beta_1\right] = -(X_1 sin\theta_0 - Y_1 cos\theta_0) + Y_{12} - X_{31}\,sin(\theta_1 + \beta) + Y_{31}cos(\theta_1 + \beta) + Y_{32} + X_{41}\,sin(\theta_2 + \beta_1) + Y_{41}cos(\theta_2 + \beta_1) + Y_{42} \quad (10)$$

https://doi.org/10.14669/AM/204802

$$I\omega + 3m[\dot{\omega}c - (u + v\omega)]c + c\left\{m(d + 2l)(\ddot{\gamma}_1 cos\varphi_1 + \dot{\gamma}_1^2 sin\varphi_1) + md[\gamma_1 cos\beta + \dot{\gamma}_1^2 sin\beta] + ml[\ddot{\gamma}_1 cos\beta + \dot{\gamma}_1^2 sin\beta] + md\left[(\dot{\omega} - \ddot{\beta})cos\beta + (\omega - \dot{\beta})^2 sin\beta\right]\right\} = a(Y_1 cos\theta - X_1 sin\theta) - Y_{12}b_{11} - c[X_{31}\sin(\theta_1 + \beta) + Y_{31}cos(\theta_1 + \beta) + Y_{32}] + c[X_{41}\sin(\theta_2 + \beta) + Y_{41}\cos(\theta_2 + \beta) + Y_{42}] \quad (11)$$

$$[I + m\ddot{\gamma}(d^2 + 2l^2)] + \left\{2ml[(\dot{v} - u\omega + c\omega^2)sin\varphi_1 + (v\omega - \dot{u} - c\omega^2)cos\varphi_1] - mdl\left[(\dot{\omega} - \ddot{\beta})cos\varphi_2 + (\omega - \dot{\beta})^2 sin\varphi_2\right]\right\} - l\{ml[\ddot{\gamma}_1 cos\varphi_3 + \dot{\gamma}_1^2 sin\varphi_3] + md[(\dot{\omega} - \ddot{\beta})cos\beta_2 + (\dot{\omega} - \ddot{\beta})sin\beta_2]\} = l[X_{31}\sin(\theta_1 + \varphi_2) + Y_{31}\cos(\theta_1 + \varphi_2)] + l_2[X_{41}\sin(\theta_2 + \beta_2) + Y_{41}cos(\theta_2 + \beta_2)] + M_1 - M_2 + M_3 \quad (12)$$

$$-(I + ml^2)\ddot{\gamma}_1 + ml_3\{[(\dot{u} - v\omega + c\omega^2)sin\beta_3 + (v\omega + \dot{u} - c\dot{\omega})cos\beta_2] - l[\ddot{\gamma}_1 cos\varphi_3 - \dot{\gamma}_1^2 sin\varphi_3]\} - lmd_4\left[(\dot{\omega} - \ddot{\beta})cos\varphi_4 + (\omega - \dot{\beta})^2 sin\varphi_4\right] = l[X_{41}\sin(\theta_{12} + \varphi_4) + Y_{41}cos(\theta_2 + \varphi_4)] + M_3 - M_4 \quad (13)$$

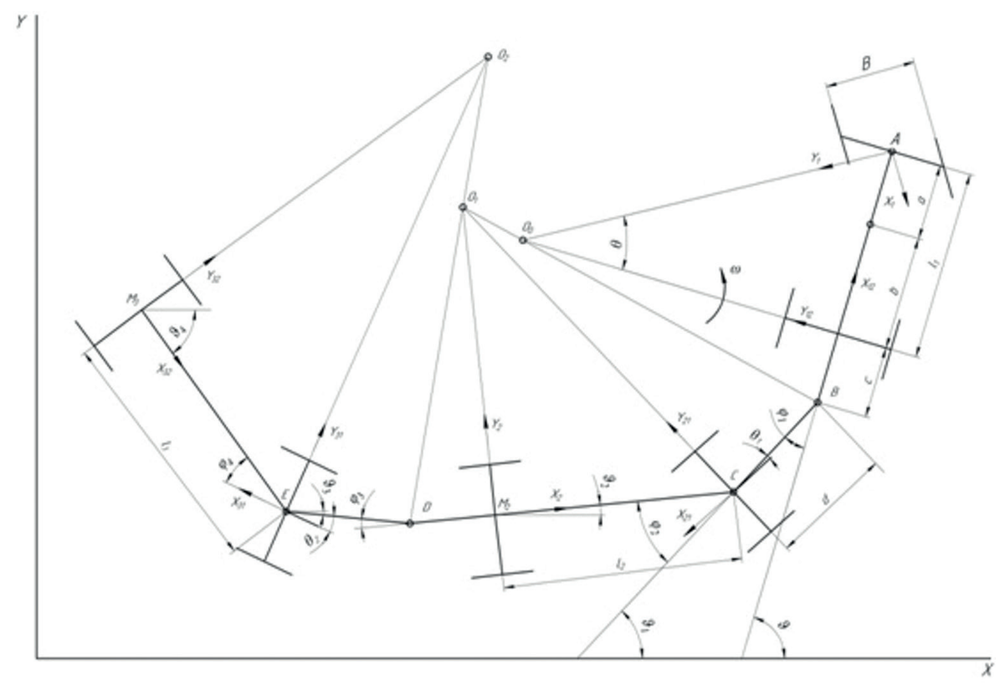

Fig. 1. Bus train consisting of three “Bohdan” buses turning diagram

To integrate the bus train motion equations, we define the necessary initial values for differential equations.

https://doi.org/10.14669/AM/204802

A. Load on bus axles.

The following assumptions were made when determining axle loads:

- the bus is evenly loaded,
- the bus centre of mass is in a vertical longitudinal plane.

The bus train in question consists of three "Bohdan A-092" buses, whose mass is $m = 8450$ kg, wheel base $l = 4.200$ m, bus length $L = 7.430$ m, bus track $B = 1.683$ m, bus width $B_w = 2.380$ m, bus height $H = 2.700$ m, coordinates $a = 2.300$ m, $b = 1.900$ m, distance from the center of mass to road plane $h = 1.320$ m, distance from the center of mass to coupling point with the second bus $c = 3.700$ m, load on front axle $G_1 = 37462$ N, on rear axle $G_i = 45348$ N.

B. Redistribution of loads on the wheels of road train axles.

$$G_{ie} = \frac{G_i}{2} + \frac{P_j h}{B} \tag{14}$$

$$G_{ii} = \frac{G_i}{2} + \frac{P_j h}{B} \tag{15}$$

where:

G_i – load on the i-th axle of the road train, N;

P_j – lateral force acting at the center of mass of the bus, N:

$$P_j = \frac{mV^2}{R} \tag{16}$$

where:

R – bus turning radius, m.

C. Bus inertia moments.

The bus central moment of inertia relative to the transverse axle was determined according to the work [14] through the inertia radius relative to the transverse axle:

$$\rho_i = \sqrt{\frac{1}{2}ab + \frac{1}{3}(H-h)h \pm \frac{1}{6}ab} \tag{17}$$

$$\rho_i = 1.876 \text{ m}$$

The bus inertia moment was determined by a known formula:

$$I_i = \rho_i^2 m_i \tag{18}$$

$$I_i = 29738.7 \text{ kgm}^2$$

D. The longitudinal forces on the bus axles are defined as:

$$P_{fi} = f_i mg \tag{19}$$

$$P_{f1} = 37462 \cdot 0.02 = 749.2 \text{ N}$$

$$P_{f2} = 45348 \cdot 0.02 = 907.0 \text{ N}$$

https://doi.org/10.14669/AM/204802

where:
f_i – the bus wheels rolling resistance coefficient, $f_i = 0.02$;
g – gravity acceleration, m/s^2.

E. The bus axles wheels lateral forces were determined by I. Rokar's hypothesis [14]:

$$Y_i = \frac{k_i \delta_i}{\sqrt{1+k_i(\varphi^2 G_i^2)^{-1}\delta_i^2}} \tag{20}$$

where:
δ_i – slip angles of the wheels of the road train i-th axle, rad;
Y_i – lateral reactions on the wheels of the road train i-th axle, N;
φ – adhesion coefficient between the tire and bearing area in a transverse direction, φ = 0.6;
k_i – lateral slip resistance coefficient, $k_1 = 85000$ N/rad, $k_2 = 170000$ N/rad (tire 215/75R17.5).

Slip angles included in expression (20) are defined by means of the bus centre of mass velocity projections and steering wheels turning angles:

- for the wheels of steered axle δ_1 and non-steered axle δ_{21} of the first bus

$$\delta_1 = \theta_0 - arctg\frac{u}{v} \tag{21}$$

$$\delta_{21} = arctg\frac{-u+b\omega}{v} \tag{22}$$

- for the wheels of steered axle δ_{31} and non-steered axle δ_{32} of the second bus

$$\delta_{31} = -\theta_1 + arctg\left(\frac{-u_2+b\omega_2}{v_2}\right) = -\theta_1 + arctg\frac{vsin\varphi_1-(u-c\omega)cos\varphi_1+d(\omega+\dot{\varphi}_1)+b(\omega+\dot{\varphi}_1)}{vcos\varphi_1+(u-c\omega)sin\varphi_1} \tag{23}$$

$$\delta_{32} = arctg\left(\frac{-u_2}{v_2}\right) = arctg\frac{vsin\varphi_1-(u-c\omega)cos\varphi_1+d(\omega+\dot{\varphi}_1)}{vcos\varphi_1+(u-c\omega)sin\varphi_1} \tag{24}$$

- for the wheels of steered axle δ_{41} and non-steered axle δ_{42} of the third bus

$$\delta_{41} = -\theta_2 + arctg[(-u_3 + b_2\omega_3)]/v_3 = -\theta_{12} + arctg\{[vcos\varphi_1 + (u - c\omega)sin\varphi_1]sin\varphi_2 - [-vsin\varphi_1(u - c\omega)cos\varphi_1 - d(\omega + \dot{\varphi}_1) - c(\omega + \dot{\varphi}_1)]cos\varphi_2 + d(\omega + \dot{\varphi}_1 + \dot{\varphi}_2)\}/\{[vcos\varphi_1 + (u - c\omega)sin\varphi_1]cos\varphi_2 + [-vsin\varphi_1(u - c\omega)cos\varphi_1 - d(\omega + \dot{\varphi}_1) - c_1(\omega + \dot{\varphi}_1)]sin\varphi_2\} \tag{25}$$

$$\delta_{42} = arctg(-u_3)/v_3 = arctg\{[vcos\varphi_1 + (u - c\omega)sin\varphi_1]sin\varphi_2 - [-vsin\varphi_1(u - c\omega)cos\varphi_1 - d(\omega + \dot{\varphi}_1) - c_1(\omega + \dot{\varphi}_1)]cos\varphi_2 + d(\omega + \dot{\varphi}_1 + \dot{\varphi}_2)\}/\{[vcos\varphi_1 + (u - c\omega)sin\varphi_1]cos\varphi_2 + [-vsin\varphi_1(u - c\omega)cos\varphi_1 - d(\omega + \dot{\varphi}_1) - c(\omega + \dot{\varphi}_1)]sin\varphi_2\} \tag{26}$$

After slip angles determination, the lateral force on the wheels of metrobus axles is found by expression (20).

https://doi.org/10.14669/AM/204802

F. The viscous friction moments in bus steering are proportional to the steered wheels turning angles [14]:

$$M_{1f} = h_{1f}\dot{\theta} \tag{27}$$

where:
h_{1f} – viscous friction coefficient in steering parts, h_{1f} = 30 Nms/rad [14];
$\dot{\theta}$ – angular velocity of steering wheels turning, rad/s.

G. The elasticity moments in bus and trailer steering are proportional to turning angles of the reduced wheels:

$$M_{p1} = \chi_1\theta \tag{28}$$

where:
χ_1 – bus steering drive stiffness coefficient, which is the torque ratio applied to the steering wheel to the turning angle of the bus locked steered wheels, $\chi_1 = 6303$ Nm/rad [14].

To find the three-link road train maneuverability and movement stability indicators in dynamic equations (9–13), the kinematic equations should be added [14]:

$$\begin{cases} \dot{x} = vcos\vartheta - usin\vartheta \\ \dot{y} = vsin\vartheta + ucos\vartheta \\ \dot{\vartheta} = \omega \end{cases} \tag{29}$$

and the equations for turning (yaw) angles of the second and third bus:

$$\theta_{1,2} = u\varphi_{1,3} \tag{30}$$

where:
u – drive control transmission ratio, which is defined as the ratio of the turning angle of the second and third buses steered wheels to the appropriate folding angles, for the bus direct drive control, $u = 0.6$ [14];
$\varphi 1$, $\varphi 2$ – folding angles of the first and second, the second and third buses, rad.

3. Results

According to UNECE Regulation 36 [8], the main indicator of vehicle maneuverability is the overall lane width during its circular movement, determined by integrating the initial system of equations (9–13).

https://doi.org/10.14669/AM/204802

The road train maneuverability indicators were determined in a circular movement, provided that the bus external position is moved along an arc of radius R_{eo} = 12.5 m. Initial conditions are additionally defined as: v_0 = 5 m/s, θ_0 = 0.375 rad.

Figure 2 shows the first bus centre of mass trajectory and the bus train overall traffic lane width.

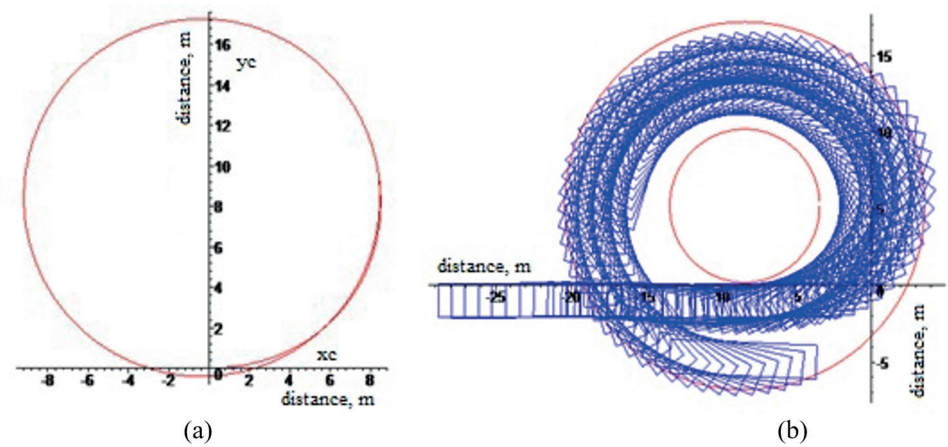

Fig. 2. The first bus center of mass trajectory (a) and bus train overall traffic lane width (b)

Analysis of graphs, Figure 2, shows that road train circular movement under mode rotation coefficient: $K_n = \dot{\theta}_0/v_0 \to \infty$ (i.e. the first bus steered wheels turn in place at an angle θ_0 = 0.375 rad) at which the maximum displacement of the trailed links is achieved, the external overall turning radius is R_{eo} = 12.5 m, the internal overall turning radius is R_{io} = 5.8 m and the overall traffic lane width is $R_{eo} - R_{io}$ = 6.7 m, significantly less than the permissible, W_o = 7.2 m, Figure 2 (b). Thus, the maneuverability of the bus train made on three "Bohdan" buses is not a limiting factor for its operation on urban routes. Therefore, consider the bus train movement stability in unsteady movement when performing various maneuvers.

When operating buses in cities, the most typical maneuver is the "lane change" maneuver, when the bus departs from a stop, makes detours, overtakes, etc. Graphic changes of buses lateral and yaw velocity, lateral acceleration when the road train performs the "lane change" maneuver at a velocity of 15 m/s, as well as changes in the maximum buses acceleration from the movement velocity are shown in Figures 3–5.

https://doi.org/10.14669/AM/204802

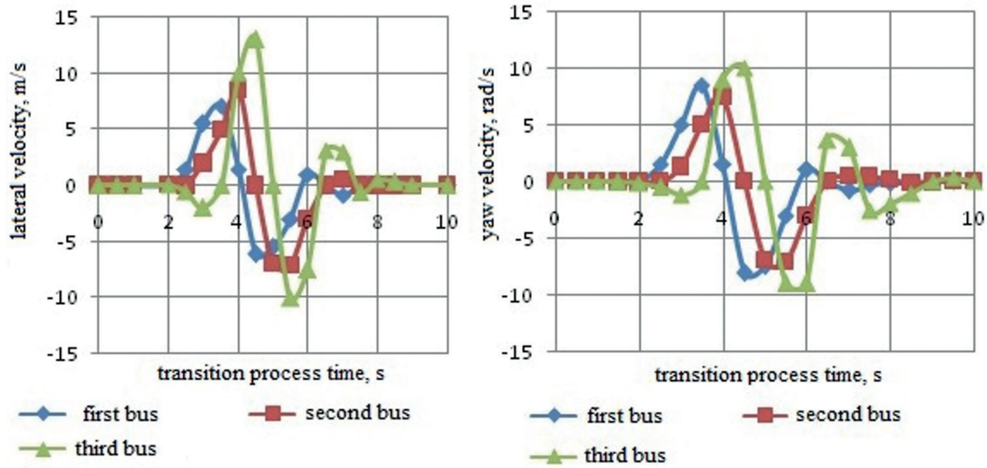

(a) (b)

Fig. 3. Change of buses lateral velocity (a) and yaw velocity (b) when the road train performs the "lane change" maneuver at a velocity of 15 m/s

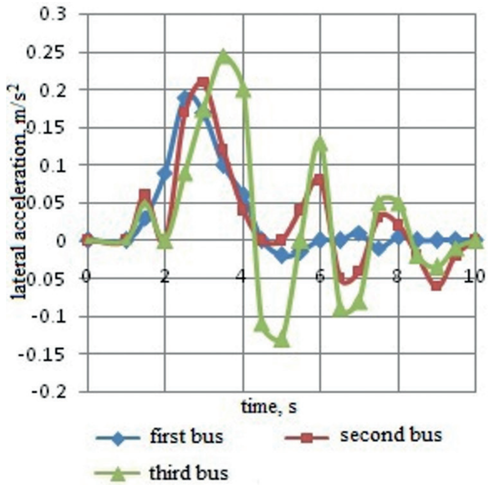

Fig. 4. Change of buses lateral acceleration when it performs the "lane change" maneuver at a speed of 15 m/s

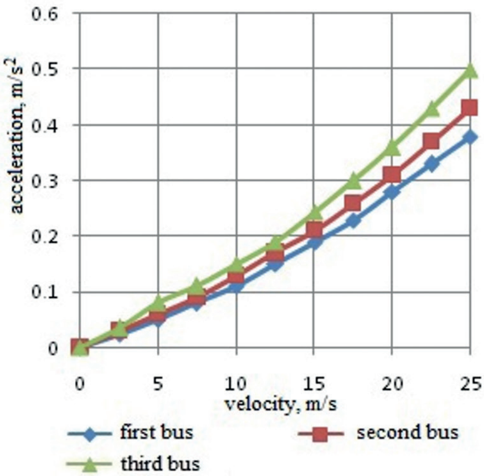

Fig. 5. Change of maximum buses acceleration from the movement velocity performing the "lane change" maneuver

Analysis of the graphs shows that the lateral velocity and yaw velosity of the buses when the road train performs "lane change" maneuver at a velocity of 15 m/s increase from the first bus to the second and third. This is because the second and third bus have smaller radius than the first. However, these velocities do not give a full picture of the bus train

https://doi.org/10.14669/AM/204802

stability, as they only qualitatively characterize the bus train behavior when it performs various maneuvers, including "lane change". According to DSTU 3310-96 [15], the length of the input part «lane change» is 24.0 m, the length of the linear part: 60 m, this is enough for the maneuver execution. Quantitatively, the bus trains stability can be measured by the lateral acceleration acting at the buses centre of mass. The change in lateral acceleration is similar to the change in lateral velocity and yaw velocity, i.e. the acceleration value from the first to the next increases. The lateral acceleration in the bus centre of mass is shown to be dependent on the road train velocity. Thus, already at a velocity of 20 m/s, the lateral acceleration of the third bus reaches a critical value of 3.6 m/s^2, i.e. the maximum velocity of the bus train should be limited to 20 m/s, Figure 5. This should be taken into account when designing the bus train and its operating criteria.

4. Discussion

Based on studies results, it was established that the maneuverability is not a limiting factor for road train operating possibility on urban routes. More questions arise when determining the movement stability, especially when road train performing different maneuvers, considering that the bus train velocity in BRT system is at 25 m/s. The comparative analysis of accelerations at the center of mass of the first, second and third buses can be used as a reference for further research in determining the movement stability according to a spatial model, that is, taking into account the bus body roll when performing various maneuveres.

5. Conclusions

Based on the existing model of a three-link articulated bus, a mathematical model of a bus train consisting of three identical buses has been developed, with which the maneuverability and movement stability indicators were determined.

It was established that during road train circular movement under mode rotation coefficient: $K_n \rightarrow \infty$ (i.e. the first bus steered wheels turn in place) at which the maximum displacement of the trailed links is achieved, the overall traffic lane width will be 6.7 m, which is significantly less than the permissible one: 7.2 m, that is, the maneuverability of the bus train made on three “Bohdan” buses is not a limiting factor for its operation on urban routes. The lateral accelerations acting at the buses center of mass depend on movement velocity when the road train performs various maneuvers, including “lane change”. It has been established that already at a velocity of 20 m/s, the lateral acceleration of the third bus reaches a critical value of 3.6 m/s^2, i.e. the maximum velocity of the bus train should be limited to 20 m/s. This should be taken into account when designing a bus train and its operating criteria.

https://doi.org/10.14669/AM/204802

6. References

[1] Catterick J, Botha T, Els S. Articulated vehicle stability control using brake-based torque vectoring on trailer using nonlinear model predictive control. SAE International Journal of Commercial Vehicles. 2023;16(1):111–126. https://doi.org/10.4271/02-16-01-0007.

[2] Chen HJ, Su WJ, Wang FC. Modeling and analyses of a connected multi-car train system employing the inerter. Advances in Mechanical Engineering. 2017;9(8):1–13. https://doi.org/10.1177/1687814017701703.

[3] Dusza M, Golofit-Stawińska M, Zboiński K. The nonlinear lateral stability of a four-axle freight car with Y25 bogies and measures to improve its faults. Applied Sciences. 2024;14(11):4545. https://doi.org/10.3390/app14114545.

[4] Galluppi O, Formentin S, Novara C, Savaresi SM. Nonlinear stability control of autonomous vehicles: a MIMO D2-IBC solution. IFAC-PapersOnLine. 2017;50(1):3691–3696. https://doi.org/10.1016/j.ifacol.2017.08.563.

[5] Gonzalez D, Perez J, Milanes V, Nashashibi F. A review of motion planning techniques for automated vehicles. IEEE Transactions on Intelligent Transportation Systems. 2016;17(4):1135–1145. https://doi.org/10.1109/TITS.2015.2498841.

[6] Gottmann F, Wind H, Sawodny O. On the influence of rear axle steering and modeling depth on a model-based racing line generation for autonomous racing. IEEE CCTA. 2018:846–852. https://doi.org/10.1109/CCTA.2018.8511508.

[7] He Y, Islam MM, Zhu S, Hu T. A design synthesis framework for directional performance optimization of multi-trailer articulated heavy vehicles with trailer lateral dynamic control systems. Proceedings of the Institution of Mechanical Engineers. Part D. Journal of Automobile Engineering 2016;231(8):1096–1125. https://doi.org/10.1177/0954407016671284.

[8] Karliński J, Ptak M, Działak P, Rusiński E. Strength analysis of bus superstructure according to Regulation No. 66 of UN/ECE. Archives of Civil and Mechanical Engineering. 2014;14(3):342–353. https://doi.org/10.1016/j.acme.2013.12.001.

[9] Ljungqvist O, Axehill D. A predictive path-following controller for multi-steered articulated vehicles. IFAC-PapersOnLine. 2020;53(2):15725–15732. https://doi.org/10.1016/j.ifacol.2020.12.053.

[10] Michalek MM. Modular approach to compact low-speed kinematic modelling of multi-articulated urban buses for motion algorithmization purposes. 2019 IEEE Intelligent Vehicles Symposium (IV). 2019:2060-2065. https://doi.org/10.1109/IVS.2019.8814281.

[11] Michałek MM, Patkowski B, Gawron T. Modular kinematic modelling of articulated buses. IEEE Transactions on Vehicular Technology. 2020;69(8):8381–8394. https://doi.org/10.1109/TVT.2020.2999639.

[12] Michałek MM, Pazderski D. Forward tracking of complex trajectories with non-standard N-trailers of non-minimum-phase kinematics avoiding a jackknife effect. International Journal of Control. 2018;92(11):2547–2560. https://doi.org/10.1080/00207179.2018.1448117.

[13] Murtagh M, Early J, Stevens G, Cunningham G, Douglas R, Best R. Modelling and control of a 96V hybrid urban bus. SAE Technical Paper. 2019:2019-01-0354. https://doi.org/10.4271/2019-01-0354

[14] Сахно ВП, Поляков ВМ, Шарай СМ, Мурований ІС, Омельницькій ОЄ. Шарнірно-зчленовані автобуси. Маневреність та стійкість: монографія. Луцьк : ІВВ Луцького НТУ. (in Ukrainian: Sakhno VP, Polyakov VM, Sharai SM, Murovanyi IS, Omelnytskyi OYe. Articulated buses. Maneuverability and stability: a monograph. Lutsk). 2021:288. https://doi.org/10.26642/ten-2022-1(89)-11-20.

[15] Дп Державтотрансндіпроект. Дсту 7434:2013 Колісні транспортні засоби. Вимоги безпеки до конструкції та технічного стану колісних транспортних засобів, двигуни яких працюють на газовому моторному паливі, та методи контролю (in Ukrainian: State Enterprise Dershavtotrans-ndiproekt. DSTU 7434:2013 Wheeled vehicles. Safety requirements for the design and technical condition of wheeled vehicles powered by gaseous fuels and methods of control). https://online.budstandart.com/ua/catalog/doc-page?id_doc=102574 (accessed on 2025 Feb 07).

https://doi.org/10.14669/AM/204802

[16] Uyulan C, Gokasan M, Bogosyan S. Hunting stability and derailment analysis of the high-speed railway vehicle moving on curved tracks. International Journal of Heavy Vehicle Systems. 2019;26(6):824–842. https://doi.org/10.1504/IJHVS.2019.102685.

[17] Vempaty S, He Y. A review of car-trailer lateral stability control approaches. SAE Technical Paper. 2017. https://doi.org/10.4271/2017-01-1580.

[18] Wang W, Li G, Liu S. Research on trajectory tracking control of a semi-trailer train based on differential braking. World Electric Vehicle Journal. 2024;15(1):30. https://doi.org/10.3390/wevj15010030.

[19] Yue M, Hou XQ, Gao RJ, Chen J. Trajectory tracking control for tractor-trailer vehicles: a coordinated control approach. Nonlinear Dynamics. 2018;91(2):1061–1074. https://doi.org/10.1007/s11071-017-3928-9.

[20] Zhang Y, Khajepour A, Huang Y. Multi-axle/articulated bus dynamics modeling: a reconfigurable approach. Vehicle System Dynamics. 2018;56(9):1315–1343. https://doi.org/10.1080/00423114.2017.1420205.